Scientific Excellence • Resource Protection & Conservation • Benefits for Canadians
Excellence scientifique • Protection et conservation des ressources • Bénéfices aux Canadiens

Continental Shelf Wave Propagation on the Labrador Shelf

S. Narayanan and I. Webster

Issuing Establishment:
Science Branch
Department of Fisheries and Oceans
P.O. Box 5667
St. John's, Newfoundland A1C 5X1

June 1989

Canadian Technical Report of Fisheries and Aquatic Sciences No. 1699

Fisheries and Oceans Pêches et Océans

Canada

Canadian Technical Report of Fisheries and Aquatic Sciences

Technical reports contain scientific and technical information that contributes to existing knowledge but which is not normally appropriate for primary literature. Technical reports are directed primarily toward a worldwide audience and have an international distribution. No restriction is placed on subject matter and the series reflects the broad interests and policies of the Department of Fisheries and Oceans, namely, fisheries and aquatic sciences.

Technical reports may be cited as full publications. The correct citation appears above the abstract of each report. Each report is abstracted in *Aquatic Sciences and Fisheries Abstracts* and indexed in the Department's annual index to scientific and technical publications.

Numbers 1–456 in this series were issued as Technical Reports of the Fisheries Research Board of Canada. Numbers 457–714 were issued as Department of the Environment, Fisheries and Marine Service, Research and Development Directorate Technical Reports. Numbers 715–924 were issued as Department of Fisheries and the Environment, Fisheries and Marine Service Technical Reports. The current series name was changed with report number 925.

Technical reports are produced regionally but are numbered nationally. Requests for individual reports will be filled by the issuing establishment listed on the front cover and title page. Out-of-stock reports will be supplied for a fee by commercial agents.

Rapport technique canadien des sciences halieutiques et aquatiques

Les rapports techniques contiennent des renseignements scientifiques et techniques qui constituent une contribution aux connaissances actuelles, mais qui ne sont pas normalement appropriés pour la publication dans un journal scientifique. Les rapports techniques sont destinés essentiellement à un public international et ils sont distribués à cet échelon. Il n'y a aucune restriction quant au sujet; de fait, la série reflète la vaste gamme des intérêts et des politiques du ministère des Pêches et des Océans, c'est-à-dire les sciences halieutiques et aquatiques.

Les rapports techniques peuvent être cités comme des publications complètes. Le titre exact paraît au-dessus du résumé de chaque rapport. Les rapports techniques sont résumés dans la revue *Résumés des sciences aquatiques et halieutiques*, et ils sont classés dans l'index annuel des publications scientifiques et techniques du Ministère.

Les numéros 1 à 456 de cette série ont été publiés à titre de rapports techniques de l'Office des recherches sur les pêcheries du Canada. Les numéros 457 à 714 sont parus à titre de rapports techniques de la Direction générale de la recherche et du développement, Service des pêches et de la mer, ministère de l'Environnement. Les numéros 715 à 924 ont été publiés à titre de rapports techniques du Service des pêches et de la mer, ministère des Pêches et de l'Environnement. Le nom actuel de la série a été établi lors de la parution du numéro 925.

Les rapports techniques sont produits à l'échelon régional, mais numérotés à l'échelon national. Les demandes de rapports seront satisfaites par l'établissement auteur dont le nom figure sur la couverture et la page du titre. Les rapports épuisés seront fournis contre rétribution par des agents commerciaux.

Canadian Technical Report of

Fisheries and Aquatic Sciences 1699

June 1989

CONTINENTAL SHELF WAVE PROPAGATION ON THE LABRADOR SHELF

by

Savithri Narayanan

Science Branch

Department of Fisheries and Oceans

P.O. Box 5667

St. John's, Newfoundland, A1C 5X1

and

Ian Webster

CSIRO Centre for Environmental Mechanics

G.P.O. Box 821

Canberra, A.C.T. 2601

Australia

90-04322/

(c)Minister of Supply and Services Canada 1989

Cat. No. Fs 97-6/1699E ISSN 0706-6457

Narayanan, S., and I. Webster. 1989. Continental shelf wave propagation on the Labrador Shelf. Can. Tech. Rep. Fish. Aquat. Sci. 1699: v + 22 p.

CONTENTS

Page

Abstract/Résumé iv

List of Figures v

1. Introduction 1

2. Model Description 1

3. Mode Separation 6

4. Downstream Boundary Conditions..... 8

5. Application to Labrador Shelf 11

6. Discussion 20

7. Summary 20

Acknowledgments 22

References 22

ABSTRACT

Narayanan, S., and I. Webster. 1989. Continental shelf wave propagation on the Labrador Shelf. Can. Tech. Rep. Fish. Aquat. Sci. 1699: v + 22 p.

A barotropic shelf wave model has been developed to analyze the low frequency response of a continental shelf to external forces such as wind stress and forces at the boundaries of the domain resulting from energy propagating into the region. The sensitivity of the model to the boundary conditions at the open boundaries and to the friction parameterization is investigated. A method of decomposing the response into dominant shelf wave modes is outlined. The model is then applied to the Labrador Shelf with wind forcing and forcing at the coastal boundary representing the Hudson Strait pumping.

RÉSUMÉ

Narayanan, S., and I. Webster. 1989. Continental shelf wave propagation on the Labrador Shelf. Can. Tech. Rep. Fish. Aquat. Sci. 1699: v + 22 p.

Pour analyser la faible réponse en fréquence d'une plate-forme continentale aux forces externes comme la tension et les forces du vent, aux limites du domaine résultant de la propagation d'énergie dans la région un modèle d'onde de plate-forme barotropique a été élaboré. La sensibilité du modèle aux conditions de limite, aux limites ouvertes et à la paramétrisation du frottement est analysé. Une méthode de décomposition de la réponse en modes d'onde de plate-forme prédominants est présenté. Le modèle est ensuite appliqué à la plate-forme du Labrador dans lequel la force du vent et les forces s'exerçant à la limite littorale représente le pompage de la baie d'Hudson.

LIST OF FIGURES

Page

Figure 1. Location diagram 2

Figure 2. The Labrador Shelf indicating the model boundary; Lines S, N and H are cross-sections along which model solutions are decomposed into CSW modes 3

Figure 3. Coordinate system and the difference scheme 5

Figure 4. Ratio in percent of the maximum ψ amplitude of the second dominant mode to the maximum mode 1 amplitude 9

Figure 5. Contours of real part of streamfunction for $\omega = 0.32$ f, (a) $r = 1.5 \times 10^{-4}$ m/s, (b) with the high friction downstream region 10

Figure 6. Bathymetry of the Labrador Shelf 12

Figure 7. Streamfunction amplitude contours for the Labrador Shelf with $\omega = 0.16$ f 14

Figure 8. Cross-shelf structures of the dominant CSW modes along line S, Saglek Bank (See Figure 2), (a) streamfunction, (b) alongshore velocity, (c) onshore velocity, (d) elevation 15

Figure 9. Alongshore velocities associated with the lowest three modes along Line N, Nain Bank 19

Figure 10. Alongshore velocities associated with the dominant modes along Line H, Hamilton Bank 21

1. INTRODUCTION

There is increasing evidence for the presence of Continental Shelf Waves (CSW's) on the Labrador Shelf (Figure 1). Garret et. al. (1985) noticed that the sea level response at Nain, Labrador, to atmospheric pressure variations at frequencies less than 0.5 cpd departed from isostacy in amplitude and phase. Wright et. al. (1987) reinterpreted the Nain sea level data and were able to show that the variations in the sea level may be due to the influence of shelf waves generated by flow through Hudson Strait onto the northern end of the Labrador Shelf.

An EOF analysis in the frequency domain of measured currents and winds from the northern part of the Labrador Shelf also revealed significant weather band variability (Webster and Narayanan, 1988). To describe these EOF's dynamically, a two-dimensional frequency domain barotropic shelf wave model was developed for the Labrador Shelf driven by wind forcing, and by oscillations propagating into the domain through the northern boundary from Hudson Strait. In this report, we describe this model and a method of decomposing the simulated circulation into dominant shelf wave modes. We also investigate the sensitivity of the model to boundary conditions and friction parameterization, and present the results from an application to the Labrador Shelf with wind forcing over the shelf and Hudson Strait outflow.

2. MODEL DESCRIPTION

The linearized shallow-water equations for a homogeneous rotating fluid, assuming the rigid lid approximation, may be written as

$$u_t - fv + g\eta_x = \frac{\tau^x}{\rho H} - \frac{ru}{H} \qquad (1)$$

$$v_t + fu + g\eta_y = \frac{\tau^y}{\rho H} - \frac{rv}{H} \qquad (2)$$

$$(Hu)_x + (Hv)_y = 0 \qquad (3)$$

where

x,y	onshore, alongshore coordinates
u,v	onshore, alongshore velocity components
t	time
η	surface displacement from static equilibrium
f	Coriolis parameter
ρ	water density, assumed constant
g	gravity
H	water depth
τ^x, τ^y	onshore, alongshore wind stress components
r	bottom friction parameter, assumed uniform in x

The model domain and the coordinate system are given in Figure 2. Assuming the u, v, η, τ^x and τ^y are harmonic in t with ω as the frequency, and defining a

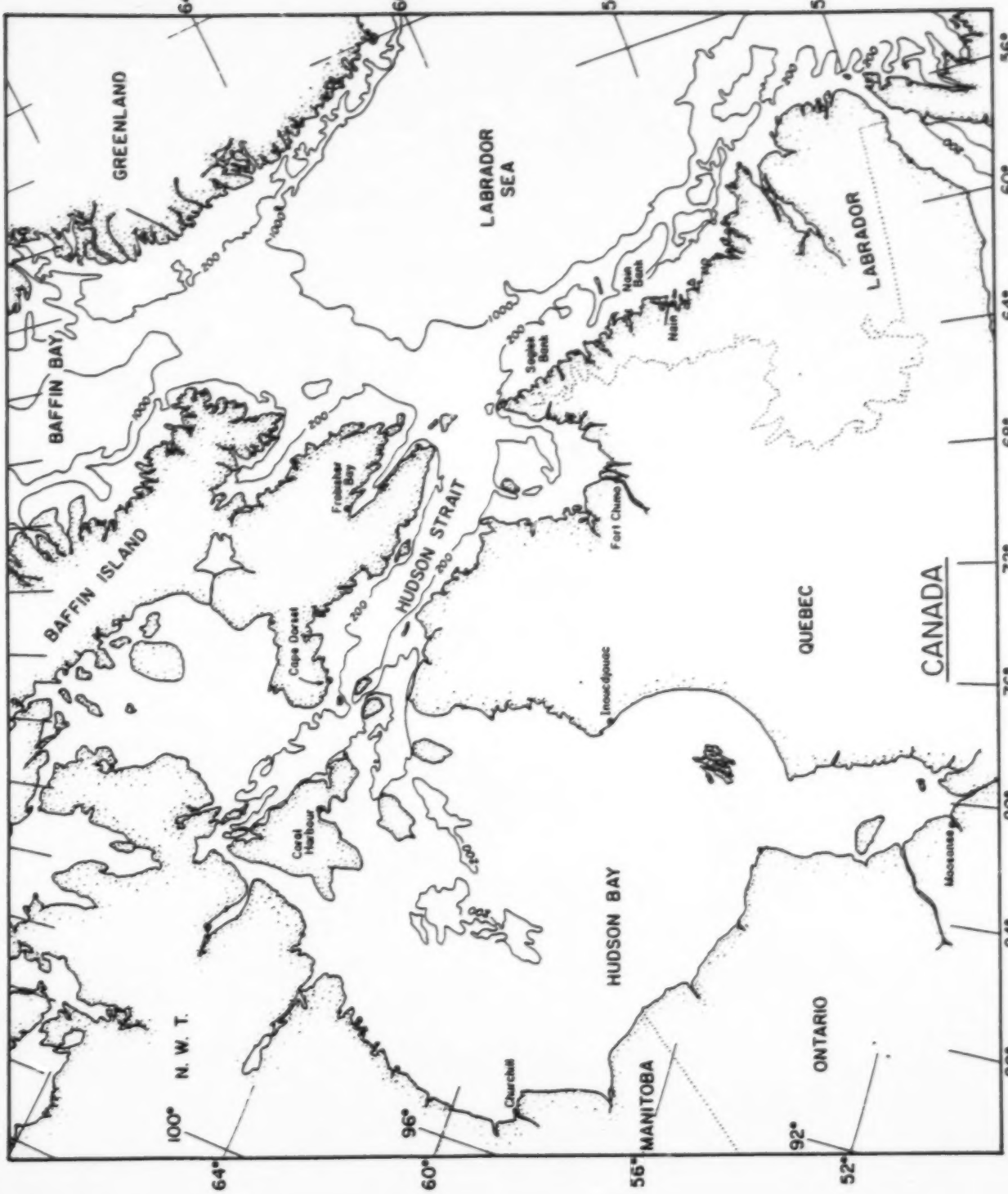

Figure 1. Location diagram.

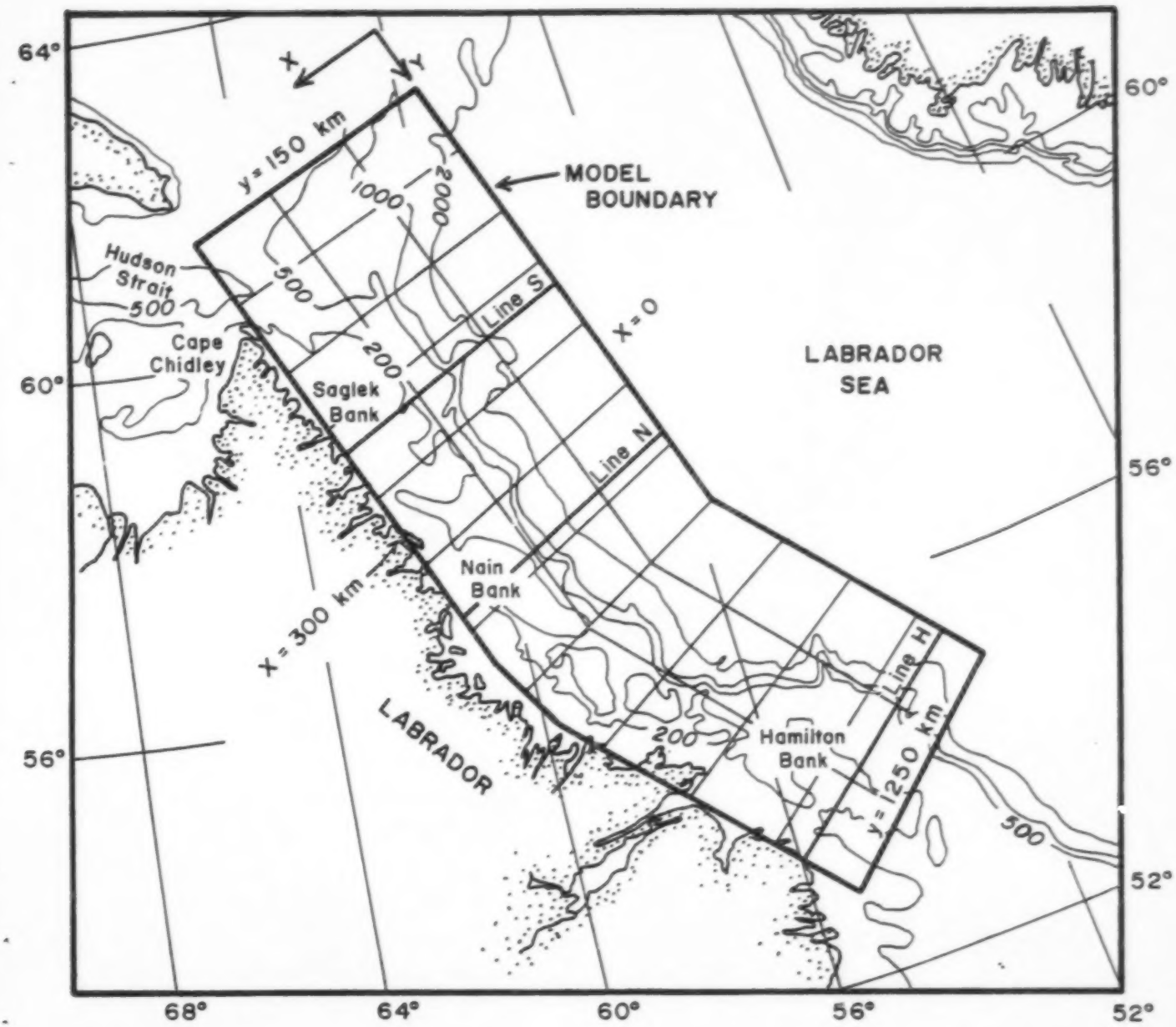

Figure 2. The Labrador Shelf indicating the model boundary; Lines S, N and H are cross-sections along which model solutions are decomposed into CSW modes.

transport stream function, ψ, such that

$$Hu = \psi_y \, e^{i\omega t}$$

$$Hv = -\psi_x \, e^{i\omega t}$$

(1) - (3) may be reduced to yield the vorticity equation in ψ as

$$\left[\left(i\omega + \frac{r}{H}\right)\frac{\psi_x}{H}\right]_x + \left[\left(i\omega + \frac{r}{H}\right)\frac{\psi_y}{H}\right]_y + \left(f\,\frac{\psi_x}{H}\right)_y$$

$$- \left(f\,\frac{\psi_y}{H}\right)_x = \frac{\tau^y}{\rho}\frac{H_x}{H^2} - \frac{\tau^x}{\rho}\frac{H_y}{H^2} + \frac{1}{\rho H}\left(\tau^x_y - \tau^y_x\right) \qquad (4)$$

Using a central difference scheme, (4) may be reduced to a set of algebraic equations in $\psi_{I,J}$ where (I,J) represent the (x,y) indices. As shown in Figure 2, the origin of the coordinate system is at the top right-hand corner of the domain.

The set of algebraic equations are then solved using the method outlined in Lindzen and Kuo (1969) where we formulate a matrix equation for each off-coast running line J (see Figure 2) as

$$\underset{\sim}{A}_J \underset{\sim}{\psi}_{J-1} + \underset{\sim}{B}_J \underset{\sim}{\psi}_J + \underset{\sim}{C}_J \underset{\sim}{\psi}_{J+1} = \underset{\sim}{D}_J \qquad (5)$$

where

$\underset{\sim}{\psi}_J$ is the vector $[\psi_{1J}, \psi_{2J} \cdots \psi_{NJ}]$

$\underset{\approx}{A}_J$, $\underset{\approx}{B}_J$, $\underset{\approx}{C}_J$ are N x N coefficient matrices

$\underset{\sim}{D}_J$ is a vector of dimension N composed of values of forcing functions at I = 1 ... N for line J

Along the upper and lower boundaries, J = 1 and M, the boundary conditions of the form $a\psi + b\psi_y = c$ with the governing equations may be reduced to yield

$$\underset{\approx}{B}_1 \underset{\sim}{\psi}_1 + \underset{\approx}{C}_1 \underset{\sim}{\psi}_2 = \underset{\sim}{D}_1 \qquad (6)$$

$$\underset{\approx}{A}_M \underset{\sim}{\psi}_{M-1} + \underset{\approx}{B}_M \underset{\sim}{\psi}_M = \underset{\sim}{D}_M \qquad (7)$$

The solution to (5) may be written as

$$\underset{\sim}{\psi}_J = \underset{\approx}{\alpha}_J \underset{\sim}{\psi}_{J+1} + \underset{\sim}{S}_J \qquad (8)$$

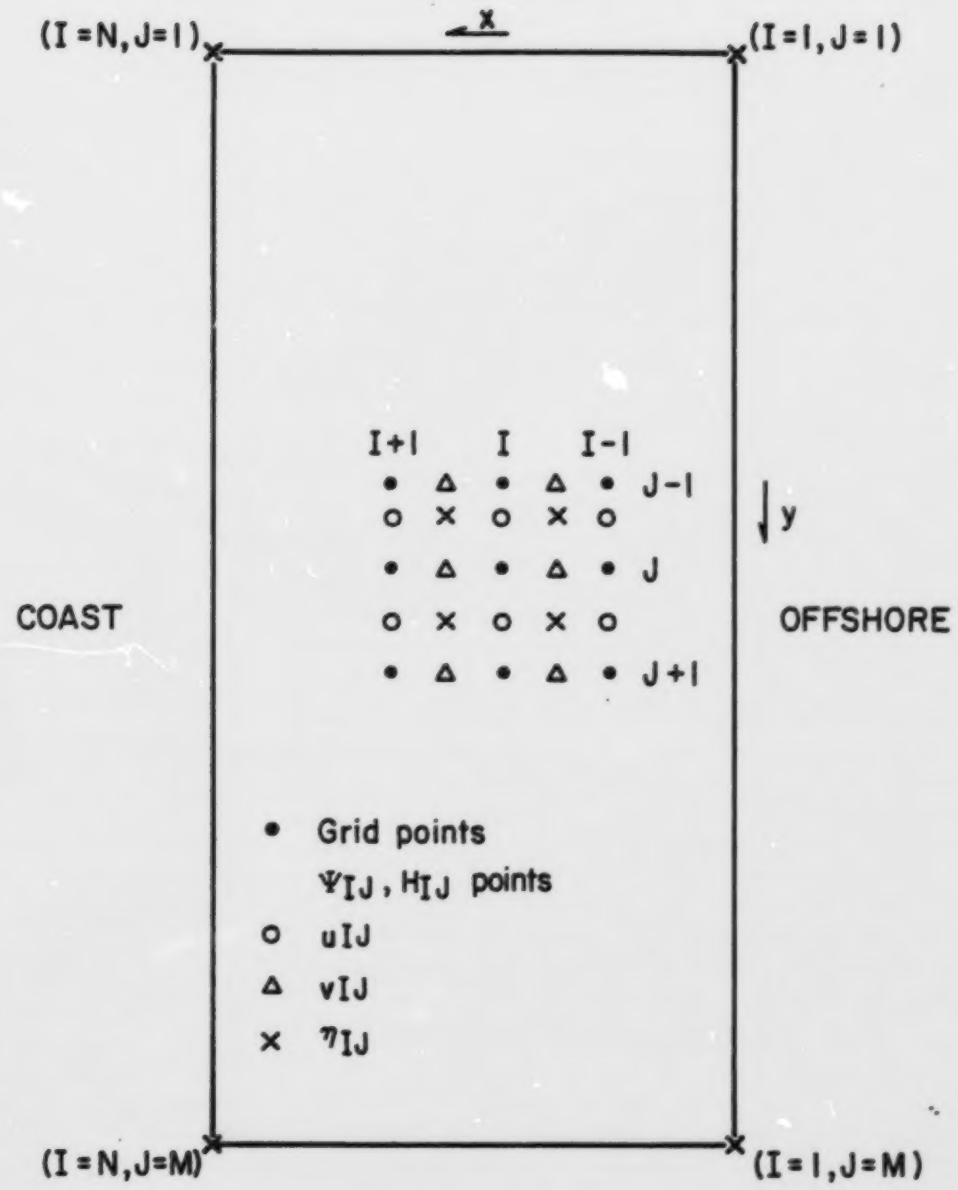

Figure 3. Coordinate system and the difference scheme.

Then,

$$\underset{\sim}{\psi}_{J-1} = \underset{\approx}{\alpha}_{J-1}\underset{\sim}{\psi}_{J} + \underset{\sim}{\beta}_{J-1} \tag{9}$$

where $\underset{\approx}{\alpha}_J$ is a N x N matrix and $\underset{\sim}{\beta}$ is a vector of dimension N.

Substituting (9) in (5), we obtain

$$\underset{\approx}{\alpha}_J = -[\underset{\approx}{A}_J\underset{\approx}{\alpha}_{J-1} + \underset{\approx}{B}_J]^{-1}\ \underset{\approx}{C}_J \tag{10}$$

$$\underset{\sim}{\beta}_J = [\underset{\approx}{A}_J\underset{\approx}{\alpha}_{J-1} + \underset{\approx}{B}_J]^{-1}\ [\underset{\sim}{D}_J - \underset{\approx}{A}_J\underset{\sim}{\beta}_{J-1}] \tag{11}$$

From (6), $\underset{\approx}{\alpha}_1$ and $\underset{\sim}{\beta}_1$ may be estimated as

$$\underset{\approx}{\alpha}_1 = -\underset{\approx}{B}_1^{-1}\underset{\approx}{C}_1$$

$$\underset{\sim}{\beta}_1 = \underset{\approx}{B}_1^{-1}\underset{\sim}{D}_1$$

Substituting back in (10) and (11), we can calculate all α's and β's. Using (9) then all ψ_J's may be estimated if ψ_M is known, that is, by applying the boundary condition (7). Note that this solution method is effectively a form of Gaussian elimination. Advantage of the Lindzen and Kuo (1969) method is that, with this method we need to invert M NxN matrices instead of one large MN x MN matrix.

As shown in Figure 3, the velocity components and the surface elevation are estimated from ψ using a staggered grid scheme. Thus

$$u_{IJ} = (\psi_{I,\ J+1} - \psi_{IJ})/\ [(\Delta y(H_{I,\ J+1} + H_{IJ})/2] \tag{12}$$

$$v_{IJ} = -(\psi_{IJ} - \psi_{I-1,J})/[\Delta x\ (H_{IJ} + H_{I-1,J})/2] \tag{13}$$

where Δx and Δy are the grid spacing in x and y directions, respectively. Since the water depth is prescribed at the ψ points, average depth values are estimated at the u,v points for (12) and (13). The η_{IJ}'s are then estimated using (1) and (2). If the surface elevation η_{11} is specified at the origin, then the x-momentum equation may be integrated to provide η_{I1} for I = 2 ...N. η_{12} is then estimated by integrating the y-momentum equation over one grid step, thus providing the boundary condition for integrating in x for J = 2. The process is repeated for all J. Thus the η solutions are arbitrary to some unspecified constant set by the choice of η_{11}. It is in fact most logical to take η_{11} = 0 since only backward propagating waves should appear at the 'backward' boundary and these have very limited influence past the edge of the shelf.

3. MODE SEPARATION

Consider a section of shelf where $h_y = 0$, that is where the shelf is uniform in the along-shore direction. Then (4) can be written as

$$\left(i\omega + \frac{r}{\bar{H}}\right)\frac{\psi_{xx}}{\bar{H}} + \left[\left(i\omega + \frac{r}{\bar{H}}\right)\frac{1}{\bar{H}}\right]_x \psi_x - \left(\frac{f}{\bar{H}}\right)_x \psi_y$$

$$= -\left(i\omega + \frac{r}{\bar{H}}\right)\frac{\psi_{yy}}{H} + \frac{\tau^y}{\rho}\frac{H_x}{H^2} + \frac{1}{\rho H}\left(\tau^x_y - \tau^y_x\right) \qquad (14)$$

Define $\gamma = i\psi_y$

and the discretized solution at a particular y as

$(\xi) = \begin{pmatrix}\psi\\ \gamma\end{pmatrix}$, where ξ is a vector of dimension 2N.

Then, (14) may be written as

$$\underset{\sim}{A}\,\underset{\sim}{\xi} = i\underset{\sim}{\xi}_y + \underset{\sim}{\tau} \qquad (15)$$

where $\underset{\sim}{\tau}$ represents the forcing term.

The homogeneous problem $\underset{\sim}{\tau} = (0)$ is

$$\underset{\sim}{A}\,\underset{\sim}{\xi} = i\underset{\sim}{\xi}_y \qquad (16)$$

Assuming wavelike propagation in the y direction ($\xi \alpha e^{-iky}$), the differential eigenvalue problem (16) reduces to finding eigenvalues k and eigenvectors $\underset{\sim}{\xi}$ of

$$\underset{\sim}{A}\,\underset{\sim}{\xi} = k\,\underset{\sim}{\xi} \qquad (17)$$

If $\underset{\sim}{\xi}^1$, $\underset{\sim}{\xi}^2$ ... $\underset{\sim}{\xi}^N$, are eigenvectors of this equation and $\underset{\sim}{\xi}$ is the vector with components $((\psi_{IJ}), I = 1,N, (i\psi_y)_{IJ}, I = 1,N)$ where ψ_{IJ} is the stream function at the grid point (I,J) corresponding to the forced problem (4), then $\underset{\sim}{\xi}$ may be expanded as a linear combination of the eigenvectors $\underset{\sim}{\xi}^n$ (the solutions of the homogeneous problem) as

$$\underset{\sim}{\xi} = \sum_{n=1}^{2N} \phi_n\, \underset{\sim}{\xi}^n \qquad (18)$$

where $\phi_n(y)$ is the amplitude of the n^{th} shelf wave contributing to the total solution. Substituting in (15)

$$\sum_{n=1}^{2N} \underset{\sim}{A}\,\phi_n\,\underset{\sim}{\xi}^n = i\,\underset{\sim}{\xi}_y + \underset{\sim}{\tau} \qquad (19)$$

An orthogonality relation for the eigenvectors $\underset{\sim}{\xi}^n$ may be obtained using the solutions of the adjoint eigenvalue problem (Morse and Feshback, 1953) which is

$$\underset{\sim}{A}^{\dagger}\,\underset{\sim}{\xi}^{\dagger} = k^{\dagger}\underset{\sim}{\xi}^{\dagger} \qquad (20)$$

where $\underset{\sim}{A}^{\dagger} = \underset{\sim}{A}^{*T}$ is the Hermite conjugate operator of $\underset{\sim}{A}$. Thus

$\left(\left(\underset{\sim}{\xi}^n\right)^\dagger\right)^* \cdot \underset{\sim}{\xi}^m = \delta_{mn}$. (17) and (19) can then be combined to give

$$\Sigma\, \phi_n k_n \underset{\sim}{\xi}^n = i\underset{\sim}{\xi}_y + \underset{\sim}{\tau} \qquad (21)$$

Taking the inner product of (21) and $\left(\underset{\sim}{\xi}^m\right)^\dagger)^*$ and using the orthogonality relation, gives

$$\phi_m = \frac{i}{k_m}\left(\left(\underset{\sim}{\xi}^m\right)^\dagger\right)^* \cdot \underset{\sim}{\xi}_y + \frac{1}{k_m}\left(\left(\underset{\sim}{\xi}^m\right)^\dagger\right)^* \cdot \underset{\sim}{\tau} \qquad (22)$$

The model decomposition involves two terms: the propagation term represented by the first expression on RHS in (22) and the 'forced' term which is the second term on the RHS of (22).

4. DOWNSTREAM BOUNDARY CONDITIONS

In applications to the Labrador Shelf or any other shelf with open boundaries, the boundary condition at an open boundary should allow maximum transmission of energy across that boundary. It is a common practice to impose the condition that the gradient of the stream function normal to the boundary is zero, that is, $\psi_y = 0$ in the coordinate system defined here. However, $\psi_y = 0$ at the downstream boundary does not make it perfectly open to forward propagating modes. As a result, backward (energy) propagating modes at shorter wavelengths as well as evanescent modes, will be generated at this boundary. Hence, the imposition $\psi_y = 0$ at the downstream boundary is based on the assumption that both types of modes generated at this boundary will be dissipated within a short distance from the generation area. The validity of this assumption was tested on a shelf which is uniform in the alongshore direction and has a cross-shelf depth profile same as that at line S in Figure 2. Two scenarios were considered: one where the friction in a 250 km region adjacent to the downstream boundary is increased linearly from the interior value of 1.5×10^{-4} m/s to 5×10^{-3} m/s at the boundary, and the second one where no high friction region is included. The high friction region is expected to dissipate the reflected modes faster thus reducing the effects of the artificial boundary on the solutions in the region of interest. The shelf circulation was forced by a mode 1 forward propagating wave incident at the upstream boundary, that is at $y = 0$. The remaining boundary conditions are

$\psi = 0$ at the coast and offshore

$\psi_y = 0$ at the downstream boundary

The shelf's response was analysed for a number of frequencies, with and without the high friction region and the results were decomposed into dominant shelf wave modes. For the case with no high friction region, the ratio in percent of the maximum ψ amplitude of the second dominant mode to the maximum mode 1 amplitude, at $y = 600$ km and 1200 km, is given in Figure 4. It is evident from this figure that at frequencies less than 0.25f, the reflected modes have amplitudes less than 1% of the mode 1 amplitude, for $y \leq 1200$ km; these modes were also found to be evanescent. This is because, at low

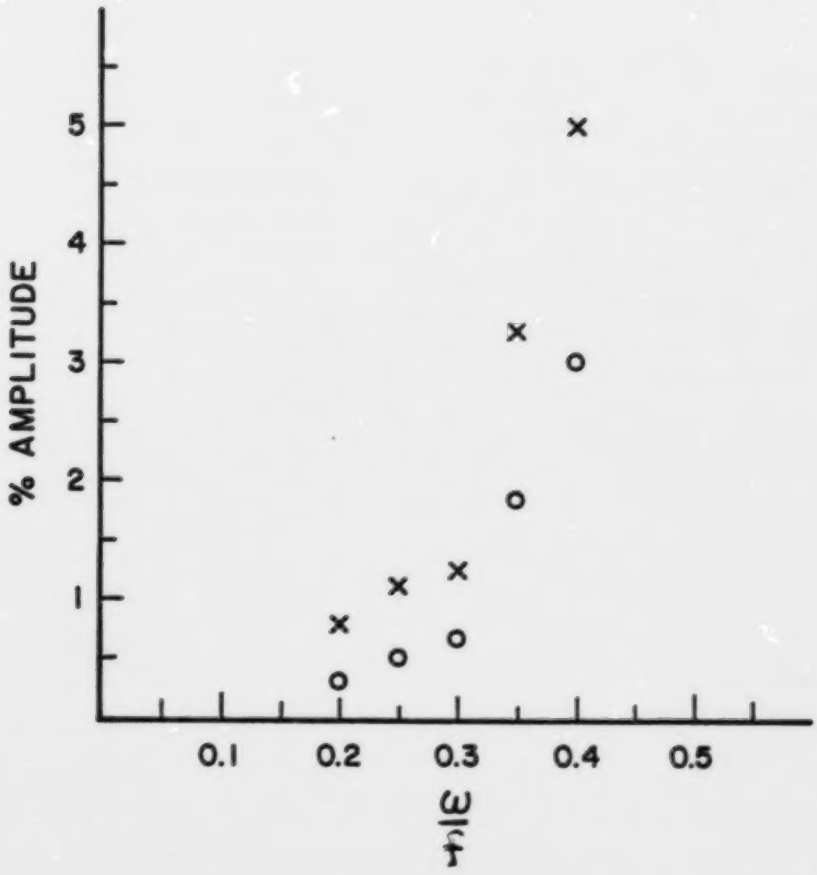

Figure 4. Ratio in percent of the maximum ψ amplitude of the second dominant mode to the maximum mode 1 amplitude.

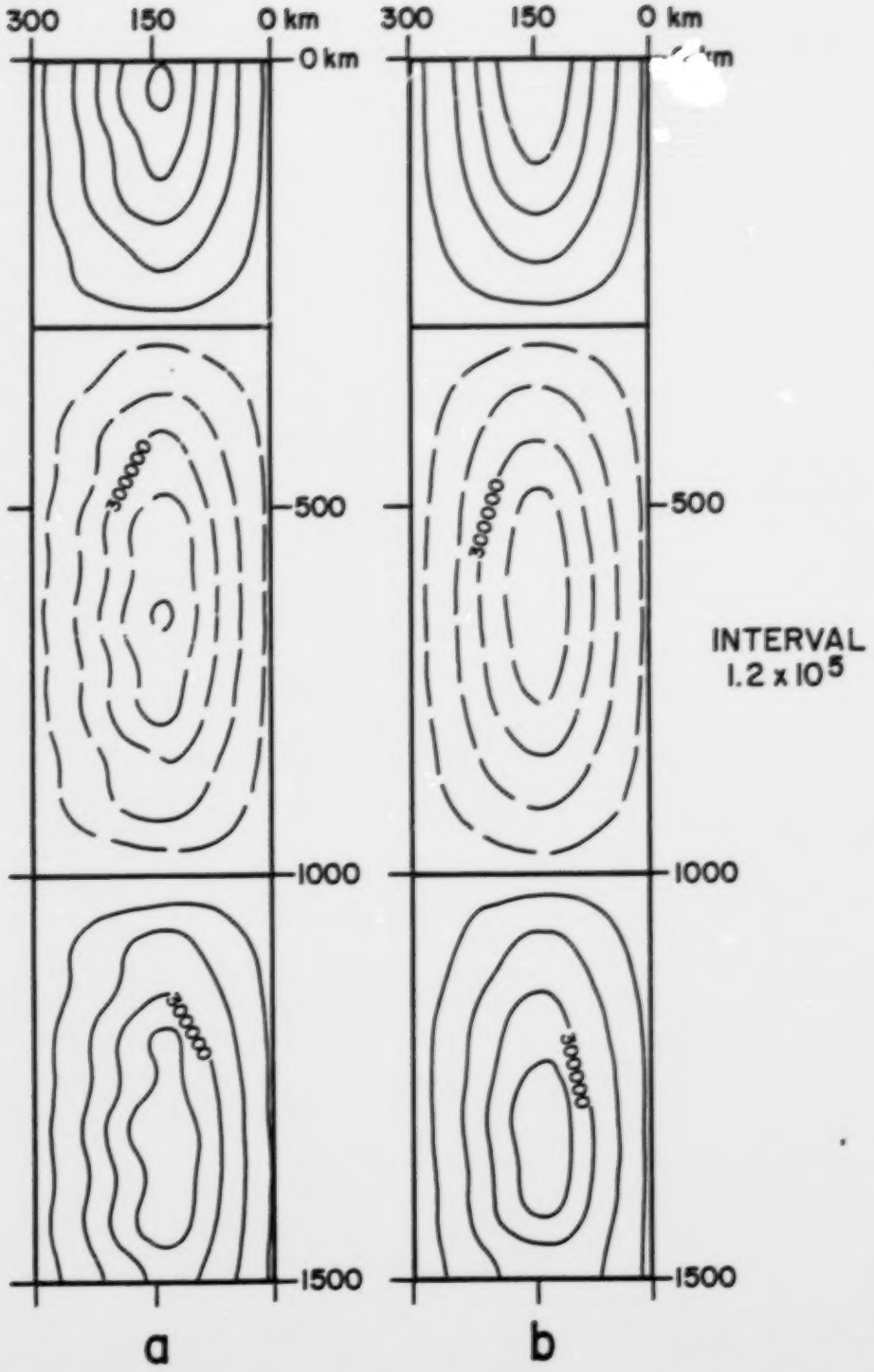

Figure 5. Contours of real part of streamfunction for $\omega = 0.32$ f, (a) $r = 1.5 \times 10^{-4}$ m/s, (b) with the high friction downstream region.

frequencies, the backward propagating modes have very short wavelengths and thus decay within a short distance of the scattering region. As the frequency is increased, the reflection also increased. Furthermore, some of the reflected energy was transported back into the region $y < 1200$ km by the backward propagating modes; energy was also transferred to evanescent modes. When the friction was increased in the region $1250 \text{ km} < y < 1500$ km, the amplitudes of the reflected modes outside the high friction region were reduced to less than 1% of the mode 1 amplitude. Furthermore, at $y = 1200$ km, the backward energy flux associated with the dominant reflected mode at $\omega = .4f$, was approximately 0.5% without the high friction region but reduced to 10^{-3}% when the high friction region is included; since energy is also transferred to the evanescent modes, the error in the solutions due to reflection could be significant. This error can be reduced considerably by increasing the friction adjacent to the downstream boundary as can be seen in Figure 5.

5. APPLICATION TO LABRADOR SHELF

The response of the Labrador Shelf (Figure 2), to winds acting over the domain and to Hudson Strait outflow are analyzed. The discretized depths between $y = 150$ km and 1250 km are determined from the actual bathymetry of the Labrador Shelf within the model domain whereas the depths between $y = 0$ and 150 km, and between 1250 km and 1500 km are extensions of the bathymetries at $y = 150$ km and 1250 km respectively. These bathymetric extensions are added to allow shelf wave energy to propagate off the Labrador Shelf at either end. Furthermore, to reduce the amount of energy propagating back onto the model domain as a result of reflection at the downstream boundary, the bottom friction is increased within the downstream extension region as in Section 4. The bathymetry discretized on a 10 km x 10 km grid, is smoothed prior to running the model, using a circular Gaussian bell having a radius of 20 km. The bathymetry used for simulations is given in Figure 6.

Mapping the actual Labrador Shelf onto the rectangular grid in Figure 2 has the effect of straightening out the coastline in its model representation. The portion of the Labrador Shelf discretized has a radius of curvature of about 2000 km, that is about ten times the width of the shelf. At mid-shelf the phase speed of a mode 1 shelf wave propagating along a 2000 km radius curved shelf having the cross-section, say at Saglek Bank, is increased by about 1% over the phase speed of this mode for a straight shelf. For mode 2, the phase speed increase is about 5%. Hence, the solution if dominated by the lower modes, will not be significantly distorted, due to transforming the shelf to a rectangular grid.

The forcing functions for the model are specified as in Webster and Narayanan (1988). The wind stress is assumed to be uniform over the shelf and equal to the phasor components coherent with the velocity EOF1 estimated from the Offshore Labrador Biological Study in 1980; in phasor form,

$$\tau^x = 0.0120 \; | \underline{-98^\circ} \text{ (Pa)}$$

$$\tau^y = 0.0663 \; | \underline{0^\circ} \text{ (Pa)}$$

at $\omega = 0.16f$.

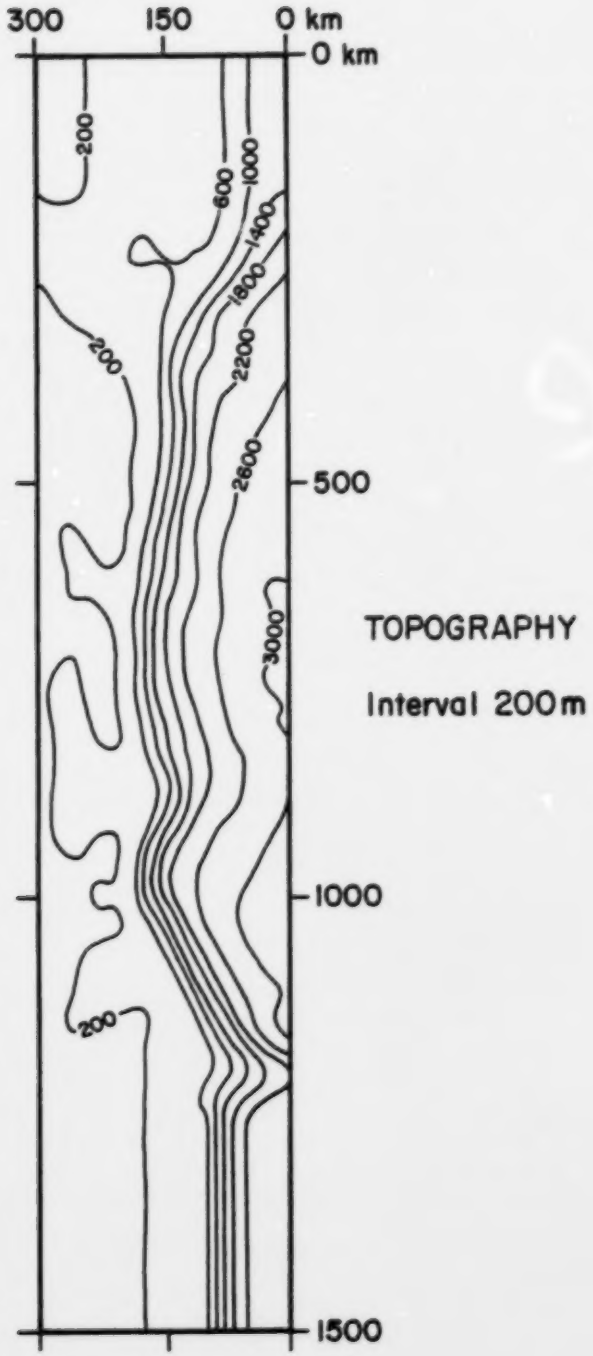

Figure 6. Bathymetry of the Labrador Shelf.

In the end sections of the domain, the wind stress forcing was linearly interpolated to zero. The Hudson Strait outflow enters the model solutions through specification of the stream function across the eastern entrance of Hudson Strait. A numerical value of $9.88 \times 10^5 \angle 52°$ (m^3/s) was specified as the net transport onto the shelf.

A no-flow condition is specified at the northern boundary, and a $\psi_x = 0$ condition is specified along the offshore boundary.

The amplitude contours of the stream function solution (Figure 7) corresponding to the discretized bathymetry of the Labrador Shelf demonstrates the influence of the flow emanating from the strait. Since not more than 10% of Hudson Strait is less than 200 m deep across its eastern entrance, the majority of the flow emanating from the Strait, by trying to follow f/H contours, tends to flow around the outside of Saglek Bank. Figure 8a shows the transport streamfunction along the cross section on Saglek Bank (Line S in Figure 2) and the first two dominant mode components estimated as outlined in Section 3; the amplitudes associated with the higher modes were too small to plot on the same diagram. Figures 8b-d show the corresponding amplitudes of the alongshore and onshore velocities and the sea surface elevations. Except for the onshore velocity which vanishes at the coast and has a maximum on the shelf, the response of the shelf adjacent to the coast is dominated by a mode 1 shelf wave with a wavelength of approximately 4680 km. Near the coast the mode 2 velocity in the alongshore direction is about 25% of that of mode 1. However, near the shelf edge, the mode 2 velocity is larger in amplitude than the mode 1. The reason for the apparent efficiency of mode 2 generation in the model can be explained using the conservation of potential vorticity argument. Much of the along-shore velocity variance for mode 2 occurs as a shelf break jet (see Fig. 8b).

As the oscillations propagate down the coast, they are modified due to the local wind forcing, due to frictional dissipation and due to the scattering of energy resulting from the alongshore variability of the shelf. Webster and Narayanan (1988) have shown that, on Nain Bank, the forcing due to "local" alongshore wind stress is approximately equal in magnitude to the forcing due to Hudson Bay barometric pressure variations whereas for Saglek Bank, the latter is the major forcing term. Hence, one can expect the wind forcing to enhance the mode 1 response as it propagates down the shelf more than a mode 2. Furthermore, the energy loss due to friction will be the lowest for mode 1 since shorter waves are dissipated faster than the longer ones.

The effects of shelf width changes on the propagation of continental shelf waves are discussed in Webster (1987). He has shown that, on a shelf maintaining a self-similar exponential shape, a mode 2 incident wave loses more energy to other modes through scattering than a mode 1. Since the shelf width at Nain Bank (Line N in Figure 2) is approximately 16% less than that at line S, the mode 2 shelf wave will lose more energy than the mode 1 as they propagate down the shelf. Hence the net effect on the two dominant modes at Saglek Bank as they propagate along the shelf will be to maintain the mode 1 as the dominant mode but to reduce the dominance of mode 2 over the higher modes. Figure 9 showing the alongshore velocities associated with the first three dominant modes demonstrates the dominance of mode 1 over other modes as well as the energy transfer to the mode 3 complex wavenumber mode; the complex wavenumber modes (evanescent modes) are non-energy propagating modes when there

Figure 7. Streamfunction amplitude contours for the Labrador Shelf with $\omega = 0.16$ f.

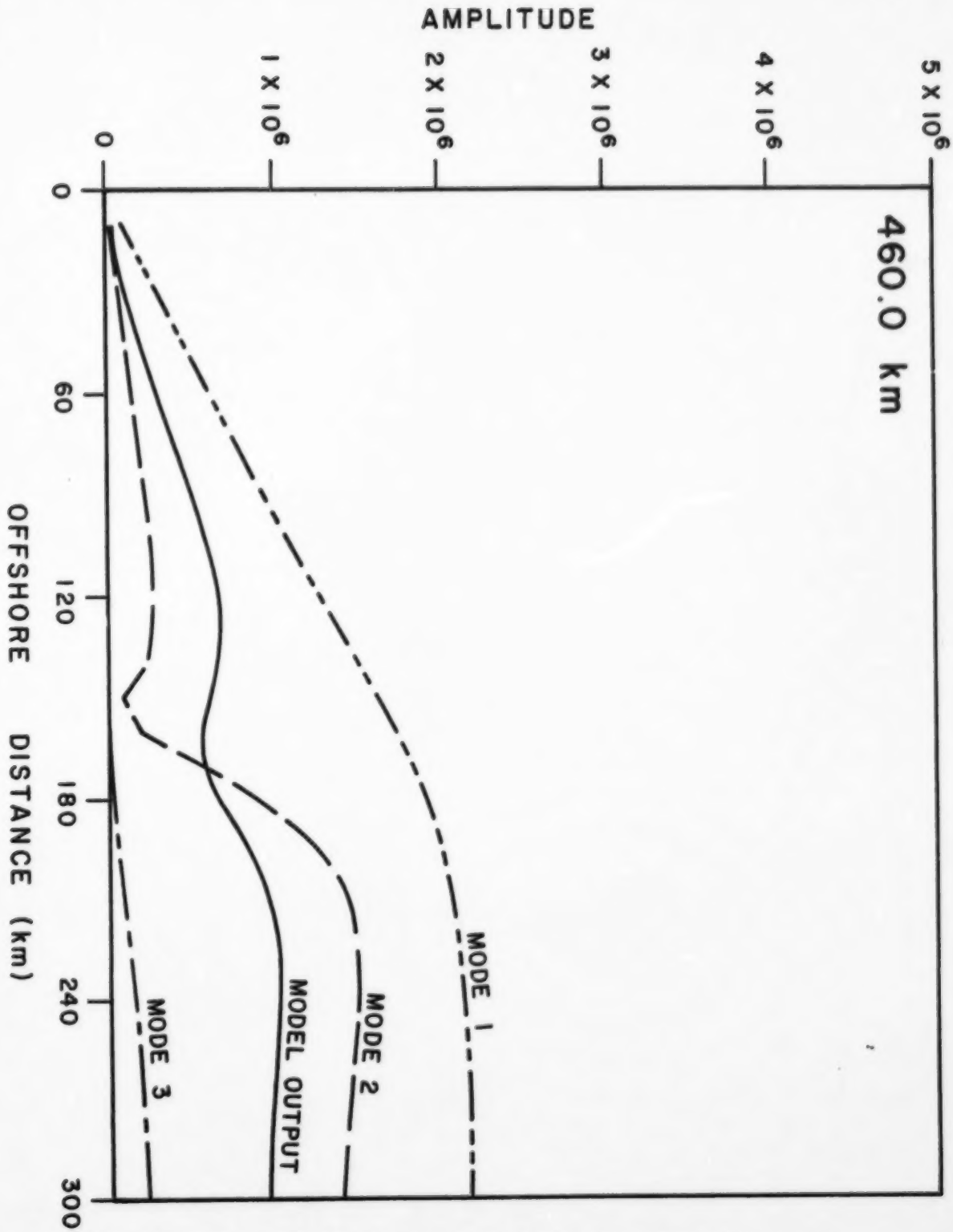

Figure 8a. Cross-shelf structures of the dominant CSW modes along Line S, Saglek Bank (See Figure 2): streamfunction.

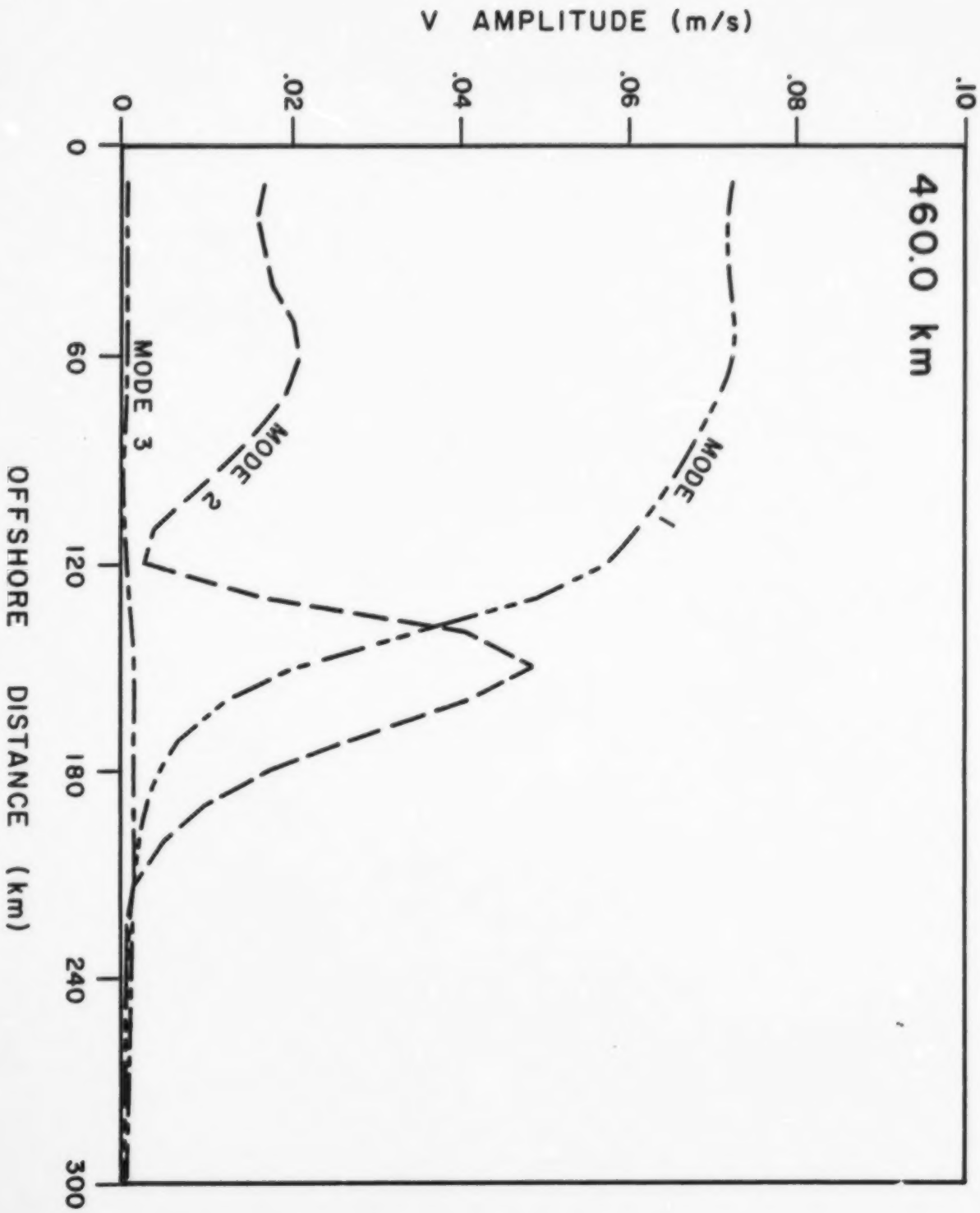

Figure 8b. Cross-shelf structures of the dominant CSW modes along Line S, Saglek Bank (See Figure 2): alongshore velocity.

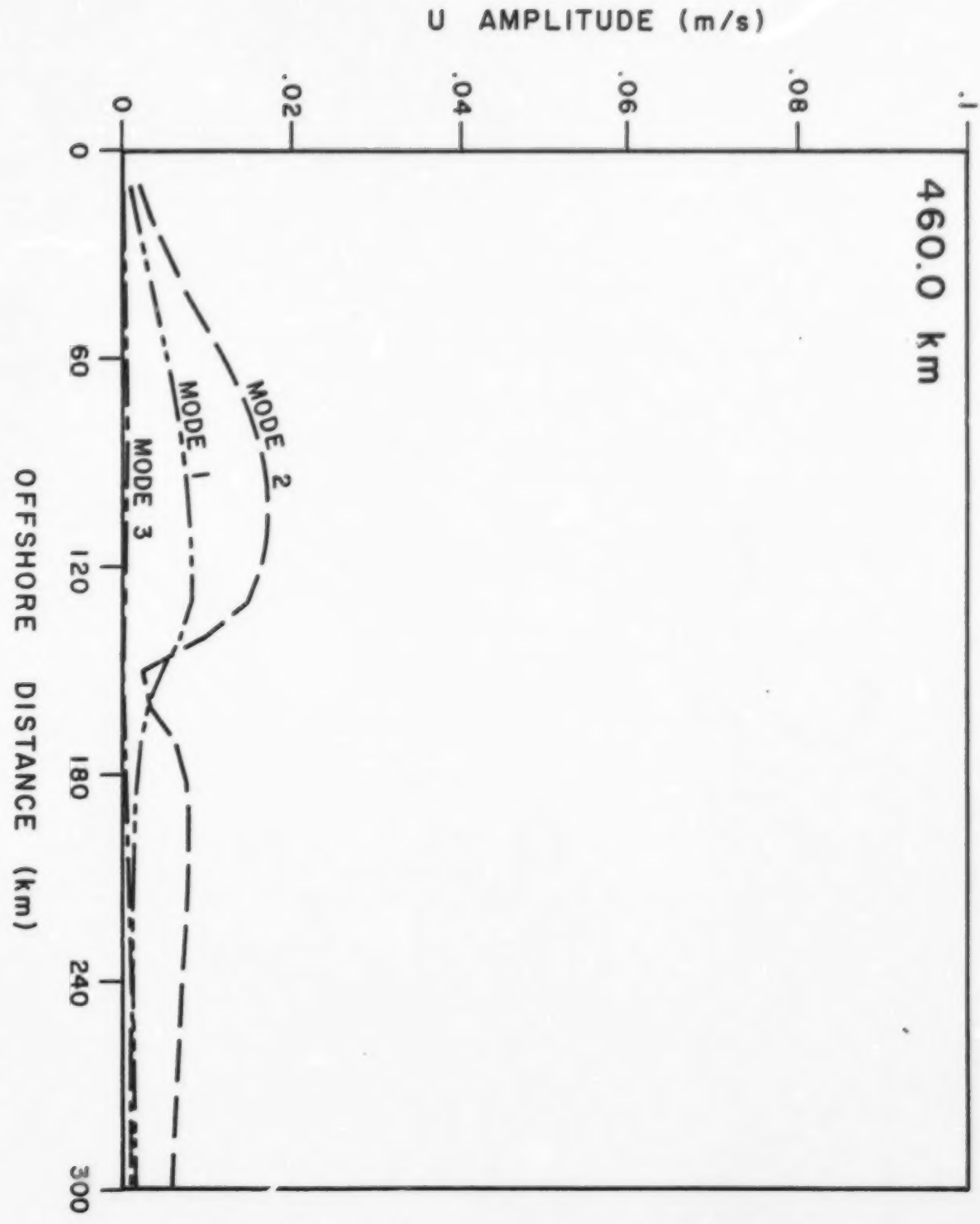

Figure 8c. Cross-shelf structures of the dominant CSW modes along Line S, Saglek Bank (See Figure 2): onshore velocity.

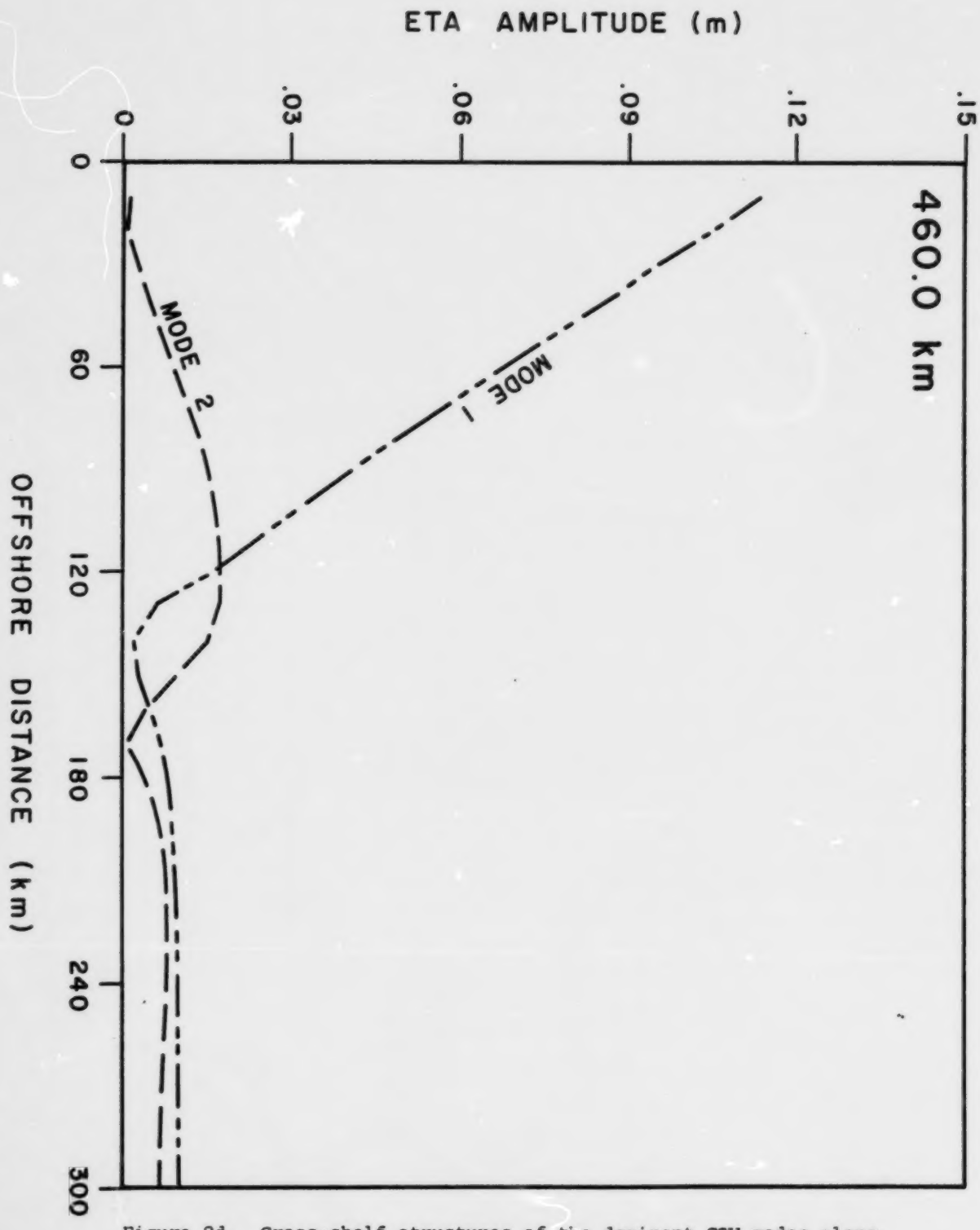

Figure 8d. Cross-shelf structures of the dominant CSW modes along Line S, Saglek Bank (See Figure 2): elevation.

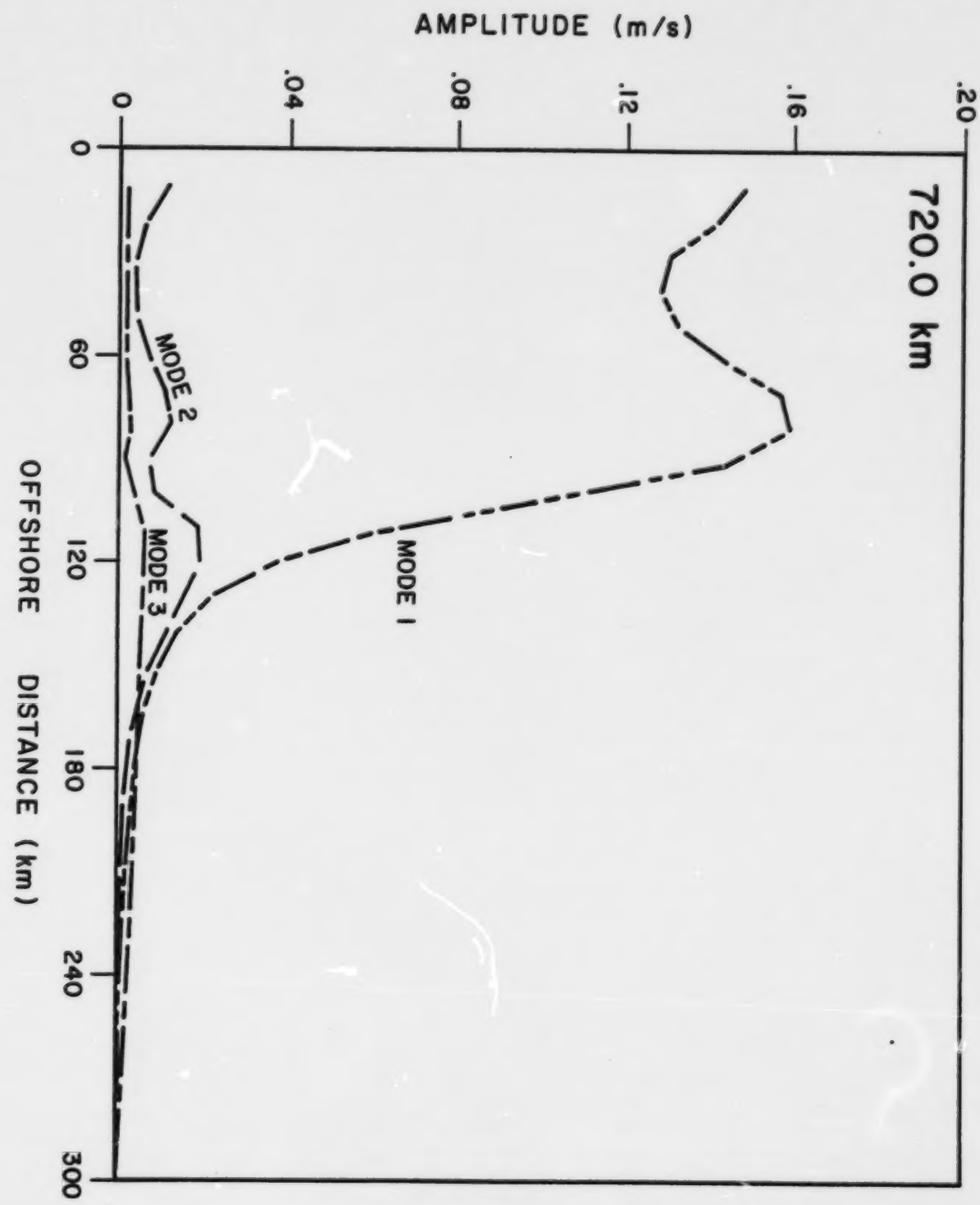

Figure 9. Alongshore velocities associated with the lowest three modes along Line N, Nain Bank.

is no friction but for the frictional case, the divergence in the energy flux associated with these modes will be exactly equal to the dissipation rate.

The 200 km section of the shelf between Nain Bank and Hamilton Bank is expected to cause considerable scattering of the incoming wave energy to smaller scales as well as to generate small scale oscillations in response to the local wind forcing. Even though the alongshore variability of the bathymetry in this region is too severe to justify the decomposition of the response to dominant shelf wave modes, such a decomposition will be more justifiable for the Hamilton Bank (line H in Figure 2). As is expected, the response at the Hamilton Bank section consists of the mode 1 and mode 2 (forward) propagating waves (Figure 10). In addition the contributions from the higher modes (the evanescent mode 3 has larger alongshore velocity amplitude than mode 2) are significant enough to be included in the analysis.

6. DISCUSSION

The model outlined here is computationally easy to use and reproduces the gross features of the barotropic response of the Labrador Shelf. The northern end of the shelf is found to respond to the regional wind forcing and the Hudson Strait pumping as an oscillation consisting of predominantly mode 1 and mode 2 shelf waves. The simulated alongshore velocities on these banks are also found to be in good agreement with the observations (Webster and Narayanan, 1988). A limitation of the model is that its resolution may not be sufficient to simulate the variability associated with narrow bathymetric features as was noted in Webster and Narayanan (1988).

The most significant shortcoming of the model is that stratification effects are not included. Stratification through interaction with topography can act as a forcing mechanism for the barotropic circulation. This effect, known as the JEBAR effect, can be included in the model with very little extra effort. Stratification can also modify the dispersion characteristics of the coastally trapped waves (Narayanan and Webster, 1988) and may allow for energy propagation by shelf modes which are non-energy propagating for a barotropic shelf. This effect will be especially significant on southern Labrador Shelf where considerable scattering of energy into shorter scale oscillations takes place.

7. SUMMARY

In this study, a two dimensional frequency-domain barotropic model has been developed to simulate the response of the Labrador shelf to external forcing. The external forcing could be (a) local wind stress or JEBAR or both (included as a forcing term in the equations), or (b) flow into the model domain as a result of oscillations propagating from upstream or due to Hudson Strait pumping (included as boundary conditions). A technique for decomposing the shelf response along a given cross section into barotropic shelf wave modes associated with that section has been developed. The principal results of this study are summarized as follows:

a. the model is capable of reproducing the gross features of the barotropic response of the Labrador Shelf to external forcing.

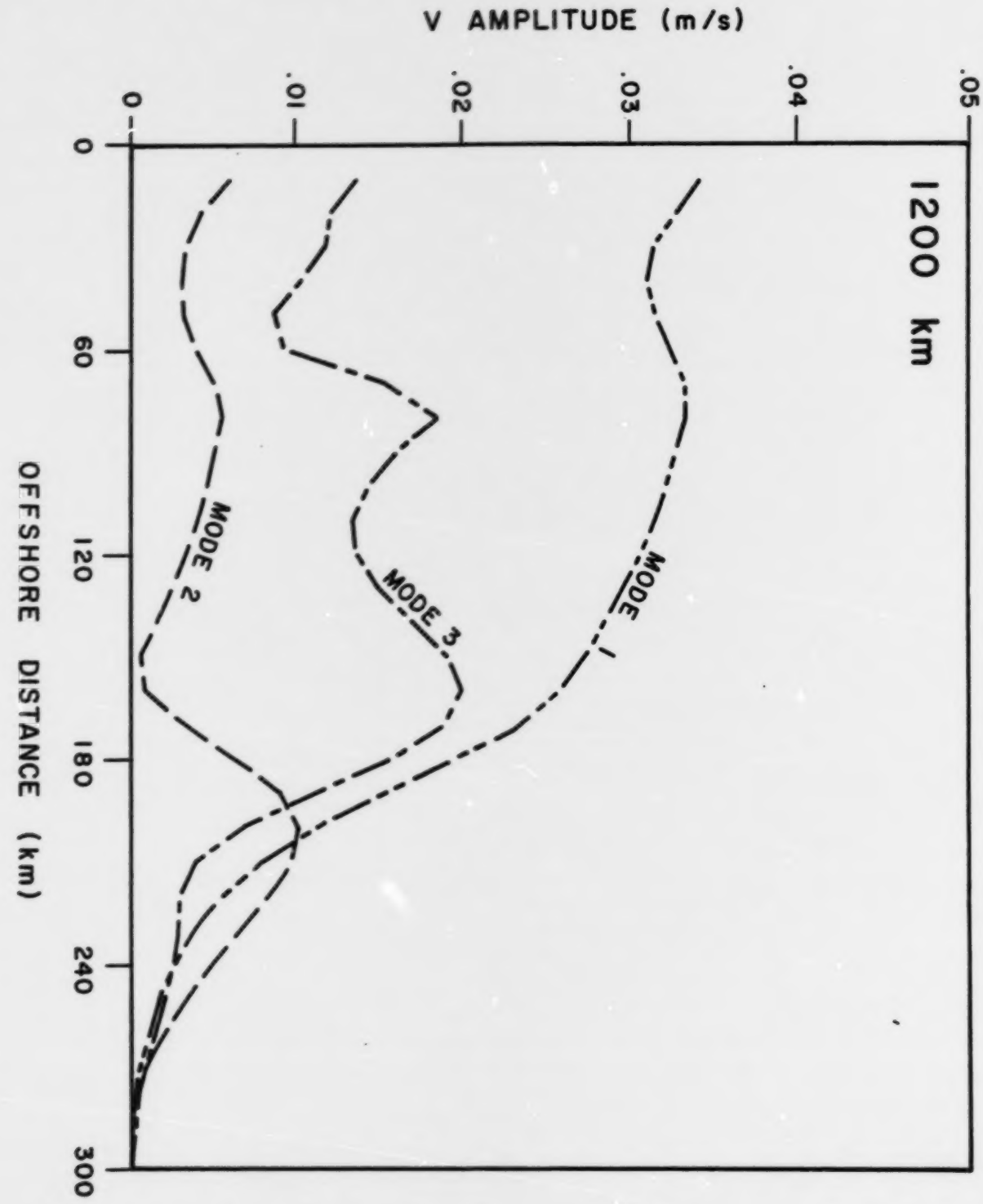

Figure 10. Alongshore velocities associated with the dominant modes along Line H, Hamilton Bank

However, to resolve the shorter length scale modifications associated with narrov bathymetric features, a localized finer resolution model may be needed.

b. The open boundary at the downstream end of the shelf is better simulated by adding a high friction region to the shelf.

c. Mode decomposition of the response on the Saglek Bank indicates the dominance of the mode 1 and mode 2 shelf waves whereas on Nain Bank, mode 1 is still dominant but the dominance of mode 2 has slightly reduced through scattering of energy to higher modes and through frictional dissipation. The high scattering region between Nain Bank and Hamilton Bank allows the generation of higher modes on Hamilton Bank.

ACKNOWLEDGMENTS

The authors wish to acknowledge the programming support provided by A. Goulding and D. Holland. Thanks are extended to D. Greenberg, J. Helbig and G. Mertz who took time to review the manuscript and provided many helpful comments and criticisms.

REFERENCES

Garrett, C., F. Majaess, and B. Toulany. 1985. Sea-level response at Nain, Labrador to atmospheric pressure and wind. Atmos-Ocean 23: 95-117.

Lindzen, R. S. and H. L. Kuo. 1969. A reliable method for the integration of a large class of ordinary and partial differential equations. Mon. Wea. Rev. 97: 732-734.

Morse, P. M. and H. Feshback. 1953. Methods of theoretical physics. McGraw-Hill, 1978 pp.

Narayanan, S. and I. Webster. 1988. Coastally trapped waves in the presence of a shelf edge density front. J. Geophys. Res. 93: 14025-14033.

Webster, I. 1985. Frictional continental shelf waves and the circulation response of a continental shelf to wind forcing. J. Phys. Oceanogr. 15: 855-864.

Webster, I. 1987. Scattering of coastally trapped waves by changes in continental shelf width. J. Phys. Oceanogr. 17: 928-937.

Webster, I. and S. Narayanan. 1988. Low-frequency variability on the Labrador Shelf. J. Geophys. Res. 93: 8163-8173.